3.20
4.6.76
111 e-1+3
plus Germany + Japan
(12)

Dis; 31

ORNL/TM-5290

Quarterly Progress Report on Fission Product Release from LWR Fuel for the Period October–December 1975

R. A. Lorenz
J. L. Collins
S. R. Manning

MASTER

OAK RIDGE NATIONAL LABORATORY

OPERATED BY UNION CARBIDE CORPORATION FOR THE ENERGY RESEARCH AND DEVELOPMENT ADMINISTRATION

Printed in the United States of America. Available from
National Technical Information Service
U.S. Department of Commerce
5285 Port Royal Road, Springfield, Virginia 22161
Price: Printed Copy $4.00; Microfiche $2.25

ORNL/TM-5290
NRC-1, -3

Contract No. W-7405-eng-26

CHEMICAL TECHNOLOGY DIVISION

QUARTERLY PROGRESS REPORT ON FISSION PRODUCT RELEASE FROM LWR FUEL FOR THE PERIOD OCTOBER-DECEMBER 1975*

R. A. Lorenz
J. L. Collins
S. R. Manning

A. P. Malinauskas, Program Manager

*This work was funded by the Nuclear Regulatory Commission under Interagency agreement 40-495-75.

NOTICE: This document contains information of a preliminary nature and was prepared primarily for internal use at the Oak Ridge National Laboratory. It is subject to revision or correction and therefore does not represent a final report.

MARCH 1976

OAK RIDGE NATIONAL LABORATORY
Oak Ridge, Tennessee 37830
operated by
UNION CARBIDE CORPORATION
for the
ENERGY RESEARCH AND DEVELOPMENT ADMINISTRATION

THIS PAGE
WAS INTENTIONALLY
LEFT BLANK

TABLE OF CONTENTS

QUARTERLY PROGRESS REPORT ON FISSION PRODUCT RELEASE FROM LWR FUEL FOR THE PERIOD OCTOBER-DECEMBER 1975

R. A. Lorenz
J. L. Collins
S. R. Manning

A. P. Malinauskas, Program Manager

SUMMARY

The series of Control Tests has been completed. These tests were conducted to evaluate the suitability of the apparatus design, to test the various fission product characterization devices and methods, and to establish the behavior of known chemical species which are expected to be encountered in the later phases of the program. Those tests which utilized either CsI or Cs_2O were found to yield deposits of hydrated CsOH in the moist environment.

With the completion of the Control Test Series, attention has been turned to the development of an acceptable method of implanting selected fission product forms into the fuel-cladding gap, and to studies of the release of such implanted species from subsequently ruptured capsules. The method of implantation which has been employed in the tests conducted thus far involves application of CsI and CsOH on UO_2 pellet surfaces from aqueous solution, and implantation of TeO_2 on the fuel pellet ends from an aqueous slurry. The tests conducted to date indicate some decomposition of CsI to yield elemental iodine, stabilization of the CsOH, probably through reaction with UO_2, migration of the tellurium to the cladding, and transport of the CsI down temperature gradients within the fuel capsules.

Two rods of a rod bundle of H. B. Robinson 2 Reactor fuel were sent to the Battelle Columbus Laboratories for gaseous species analysis and for fabrication into test capsules for this program. These capsules have been received and are currently in storage at ORNL.

Although problems had been encountered in attempts to calibrate a Knudsen cell-mass spectrometer apparatus for use in limited studies of Cs vapor pressure over UO_2, these difficulties appear to have been resolved.

---

1. INTRODUCTION

The primary objectives of the program are to determine the quantities of radiologically significant fission products which can be released under postulated spent fuel transportation accident (SFTA) and successfully terminated loss of coolant accident (LOCA) conditions, and to identify these species with respect to both chemical and physical form. Toward these ends, an apparatus has been designed and constructed and is currently being utilized in a program of research which consists of a progression of experiments which ultimately involve the use of high-burnup, light water reactor (LWR) fuel rod segments.

The first series of experiments in this progression was designed to demonstrate the adequacy of the experimental apparatus and to test the suitability of the fission product characterization devices and techniques.[1] These tests included experiments with I_2, CH_3I, CsI, and Cs_2O. The results of most of these so-called control experiments have been reported previously,[1,2] and the concluding test is described in this report.

During the conduct of the Control Test Series, a parallel effort was underway to develop a technique to implant likely fission product species in the fuel-clad gap in a manner which would simulate the distribution in irradiated fuel reasonably well. The procedure selected involves the application of water-soluble candidate fission product forms (e.g., CsI, CsOH) to the UO_2 fuel pellet surfaces from an aqueous solution. For water-insoluble species (e.g., TeO_2), on the other hand, the material is deposited in the dished ends of the pellets from an aqueous slurry.

The Implant Test Series was initiated shortly after the completion of the Control Test Series. These tests, which are directed toward a determination of the effects of clad failure size on fractional release, of atmosphere (particularly H_2O and H_2) on chemical behavior, and of simulant migration in the fuel rod, are being conducted with the apparatus shown in Fig. 1; this design differs only slightly from that described previously.[3]

As is indicated in Fig. 1, the fuel rod is induction-heated inside the furnace tube, and the rod ruptured by applying argon pressure. The first component of the collection-characterization system is a gold foil-lined thermal gradient tube; species with dewpoints above 125°C are deposited in this region. Beyond the thermal gradient tube is positioned a cascade impactor; this device separates particulates into five particle size fractions on Teflon membranes which can be removed to allow direct examination of the deposited material. High-efficiency

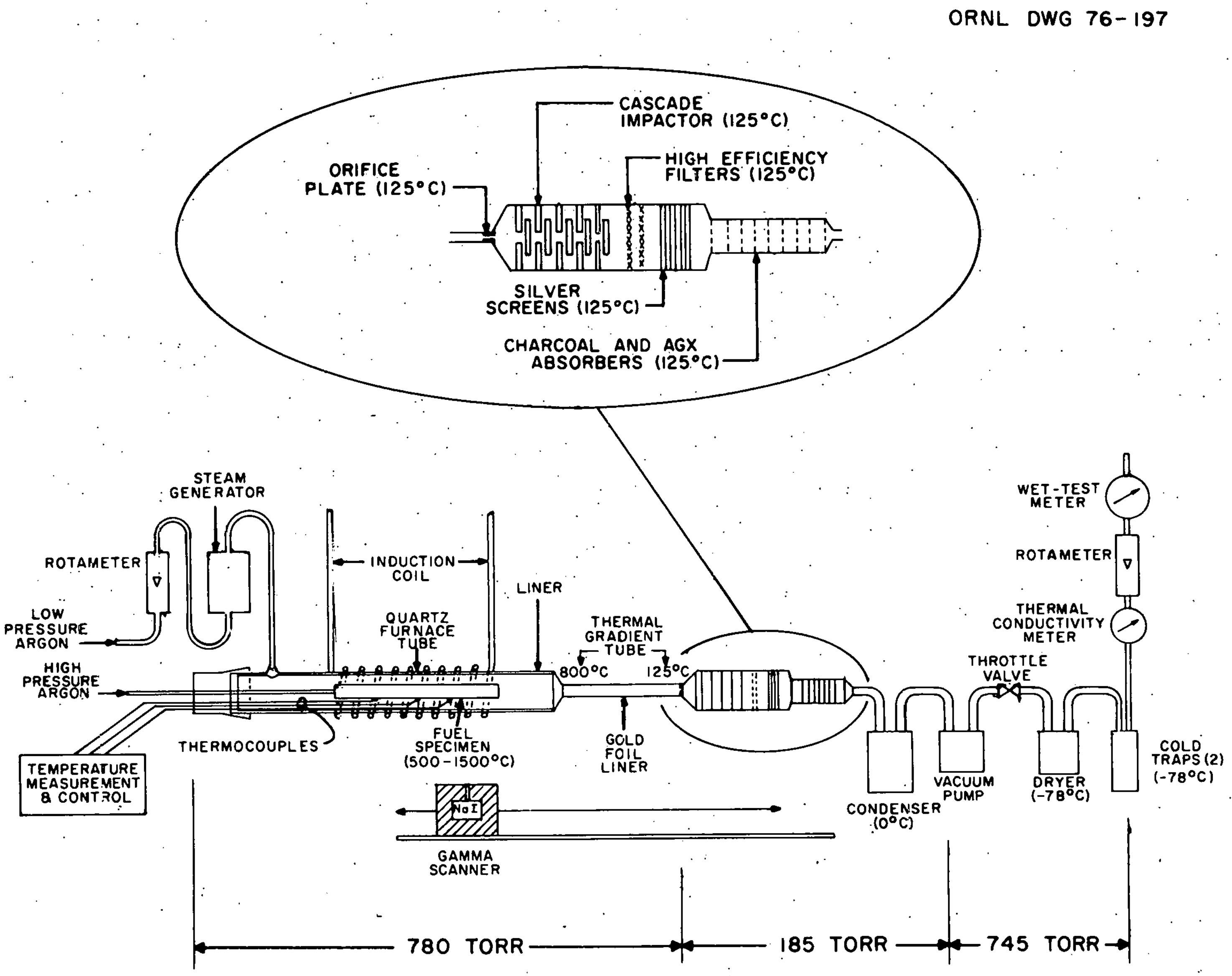

Fig. 1. Apparatus for studies of fission product release from LWR fuel rod segments.

filters complete the collection of particulates. Reactive iodine forms, such as I_2 and HI, are collected on fine-mesh silver screens, whereas less reactive forms, notably CH_3I, are collected on charcoal adsorbers and silver-exchanged zeolite beds. The apparatus is also equipped with cold traps which may be used to collect fission product noble gases. Lastly, hydrogen which is produced from the steam-Zircaloy reaction is monitored using either a thermal conductivity meter or, for larger amounts, a wet-test meter.

2. CONTROL TESTS

2.1 Cesium Oxide Behavior (Control Tests 7, 8, and 9)

Control Tests 7, 8, and 9, which were performed to study Cs_2O behavior in an 80% steam-20% argon atmosphere at 700, 800, and 950°C, have been described previously.[2] However, at that time identification of the X-ray diffraction patterns of deposits taken from the various apparatus components was not possible, owing to the lack of reference standards. We have since prepared the necessary reference materials and on this basis were able to identify the monohydrate $CsOH{\cdot}H_2O$ and higher hydrates $CsOH{\cdot}xH_2O$. (The latter species are readily formed upon exposure of the monohydrate to normal air.)

In Control Test 8, these hydrates were identified in deposits in the quartz furnace tube and on the second impactor stage. In Control Test 9, these species were identified in deposits within the thermal gradient tube. The apparently unstructured cesium deposition profile which was obtained in the thermal gradient tube from Control Test 9 is presented in Fig. 2.

Deposits taken from the furnace tubes at the conclusion of Control Tests 7 and 9 yielded distinctive X-ray diffraction patterns of considerable complexity that could not be identified. However, we believe these deposits to be primarily mixtures of cesium silicates.[4]

2.2 Cesium Iodide Behavior (Control Test 10)

Control Test 10 was conducted with a Cs-134, I-130 traced CsI sample which was placed in a quartz boat and positioned in the center

ORNL DWG 76-138 R1

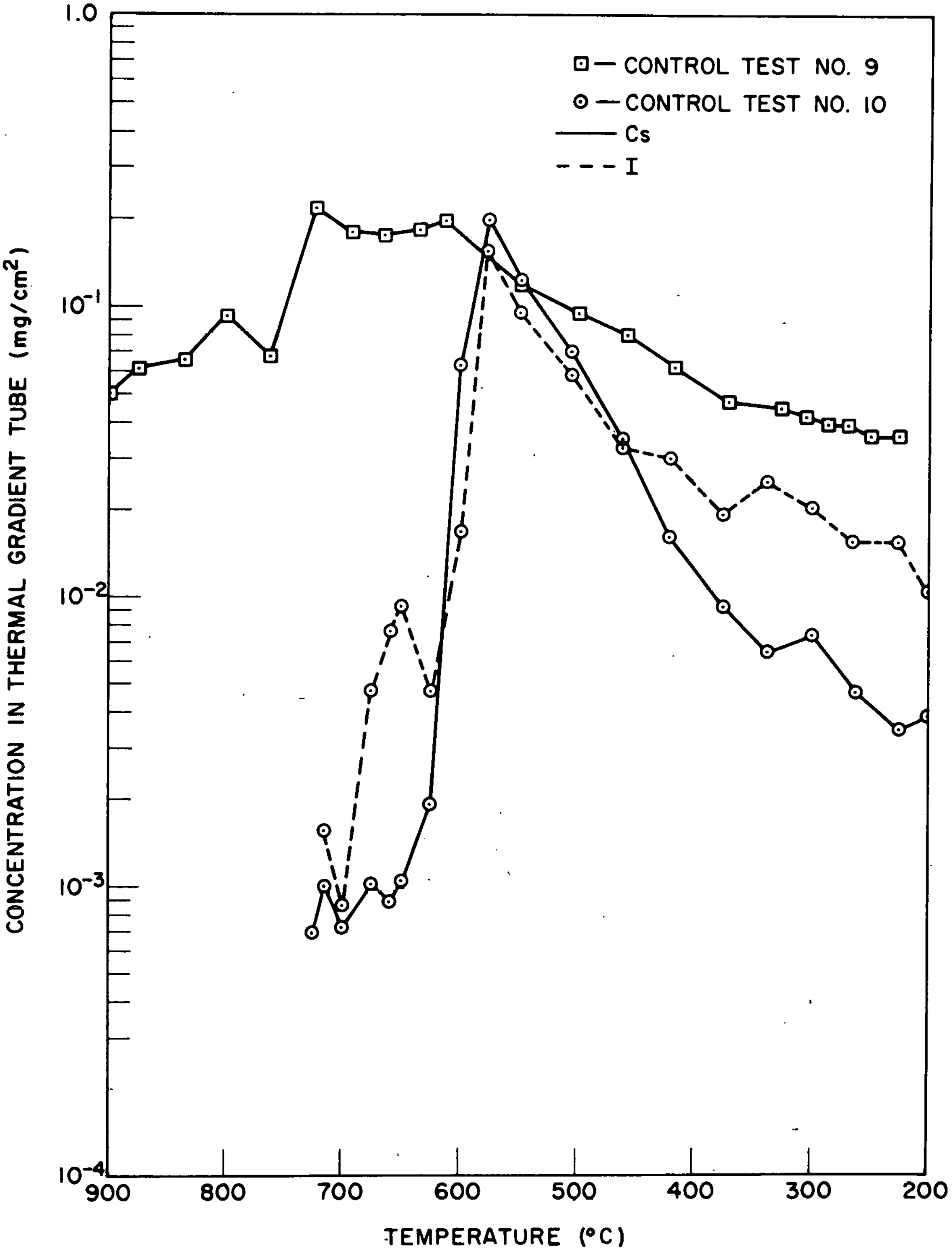

Fig. 2. Cesium-134 and iodine-130 nuclide concentration profiles in the thermal gradient tube after Control Tests 9 and 10.

of the furnace tube. The sample was rapidly brought to 700°C under reduced argon flow, then the argon flow was increased and steam injection initiated. The actual operating conditions are summarized in Table 1.

The distributions of both the cesium and the iodine nuclides are presented in Table 2. While most of the cesium remained in the furnace or was deposited in the thermal gradient tube, approximately one-third of the iodine (probably as elemental iodine) was carried into the impactor and deposited either on the aluminum surfaces of the impactor housing or on the silver screens. The cesium associated with the quartz boat was probably present as silicates. X-ray diffraction patterns which were obtained from material deposited on the third and fifth stage collectors in the impactor indicated that about 75% of the material was CsOH and the remainder CsI. On the basis of these observations, we conclude that approximately one-third of the CsI was decomposed to form I_2, cesium silicates, and CsOH.

The radioactive iodine deposited in the furnace tube was located at the cooler (about 200°C) inlet end. We believe that the iodine which deposited at the cool inlet end occurred as CsI during the first few minutes by convective gas flow within the furnace tube before the steam flow started.

As is readily apparent from the data presented graphically in Fig. 2, both the cesium and the iodine nuclide concentration profiles in the thermal gradient tube show structure which strongly suggests deposition as CsI.

Iodine-130 activities in the thermal gradient tube and on the first silver screen are presented as functions of time in Fig. 3. Almost two-thirds of the iodine which was collected by the silver screen was deposited virtually instantaneously with steam injection, and the remainder accumulated at a rate of about 0.7% per minute. In contrast to the behavior observed on the silver screen, collection of the CsI in the thermal gradient tube proceeded much more slowly; as seen from the data displayed in Fig. 3, about 75% of the CsI was deposited over a 15-minute interval, and collection appears to have been complete at the termination of the test.

Table 1. Summary of experimental operating conditions

	Experiment number			
	Control 10	Implant 1	Implant 2	Implant 3
Mass Cs (mg)	2.16	2.50	0.034	7.23
Mass I (mg)	2.06	2.39	0.033	0.70
Mass Te (mg)	0.0	0.0	0.0	1.68 ± 0.47
Vacuum drying	None	a	a	a
Pretreatment	None	b	b	b
Avg. rate of heatup (°C/sec)	0.45	0.65	11.	1.1
Time at temperature before rupture (min-°C)	-	(12-700)	(17.5-700)	(2.5-900)
Pressure at rupture (psig)	-	330	330	250
Size of rupture (mm)	-	0.046x9.0	0.06x3.6	0.23x3.5
Wall thinning	-	c	c	None
Temperature after rupture (°T)	700	700	700	900
Time at temperature (hr)	1.0	1.0	1.5	2.0
Steam flow rate (cm^3/min, STP)	277[d]	348	305	311
Argon flow rate, (cm^3/min, STP)	52[d]	60	56	56
Furnace tube pressure (torr)	750	755	735	745
Impactor pressure (torr)	186	186	186	191

[a] 30 min at 200°C, vacuum pump.

[b] 16 hr at 400°C, 1 atm argon.

[c] Flat spot 5.1 cm (2.0 in.) long; thinnest points 0.023 cm (0.009 in.).

[d] Steam and argon inflow rates; only 41% of the expected condensate volume was collected, indicating a leak in the system, probably at the furnace tube cap.

Table 2. Distributions of cesium and iodine in cesium iodide experiments

Location	Temperature (°C)	Percent of total found in each location					
		Control 1C		Implant 1		Implant 2	
		Cs	I	Cs	I	Cs	I
Quartz boat	700	23.3	1.6	-	-	-	-
UO_2 pellets	700	0	0	68.3	48.6	51.6	36.7
Zircaloy cladding	700	0	0	19.0	31.8	41.1	46.8
Quartz furnace tube	700	40.1	32.8	11.5	17.1	7.2	1.1
Thermal gradient tube	700–150	34.0	30.9	0.9	1.1	0.11	1.4
Orifice assembly	125	1.0[a]	1.8[a]	0.02	0.13	0.005	1.2
Impactor housing	125	0.78[a]	10.0[a]	0.1	1.0	0.03	6.4
First stage paper		0.04	0.09	0.01	0.03	0.002	0.05
Second stage paper		0.04	0.12	0.01	0.01	0.002	0.003
Third stage paper		0.13	0.47	0.01	0.01	0.002	0.01
Fourth stage paper		0.13	0.18	0.01	0.005	0.001	0.01
Fifth stage paper		0.40	0.26	0.03	0.03	< 0.001	0.002
Filter housing	125	0.02[a]	1.1[a]	0.003	0.02	0.001	0.81
First filter paper		0.41	0.13	0.05	0.02	<0.001	0.09
Second filter paper		0.002	0.17	<0.001	0.001	0.0	0.09
Third filter paper		0.001	0.04	-	-	0.0	0.03
Silver screen No. 1		0.005	17.9	0.0	0.13	<0.001	3.8
Silver screen No. 2		<0.001	0.37	<0.001	0.01	<0.001	0.24
Silver screen No. 3–No. 12		<0.002	0.41	<0.001	0.03	<0.001[b]	0.61[b]
Adsorber housing	125	0.0	0.0	0.0	0.0	0.001	0.01
Charcoal No. 1		0.0	0.37	<0.001	0.02	<0.001	0.83
Charcoal No. 2		0.0	0.004	0.0	<0.001	0.0	0.001
Other adsorbers		0.0	0.0	0.0	0.0	<0.001	0.01
Condenser housing	0	0.0	0.0	0.06	0.01	0.003	0.03
Condensate		0.0	0.0	0.0	<0.001	0.0	0.0
Freeze trap	-78	0.0	0.0	0.0	0.0	<0.001	0.0
Cold charcoal trap	-78	0.0	0.0	0.0	<0.001	0.0	0.0

[a] 175°C.
[b] No. 3 through No. 8.

ORNL DWG 76-147

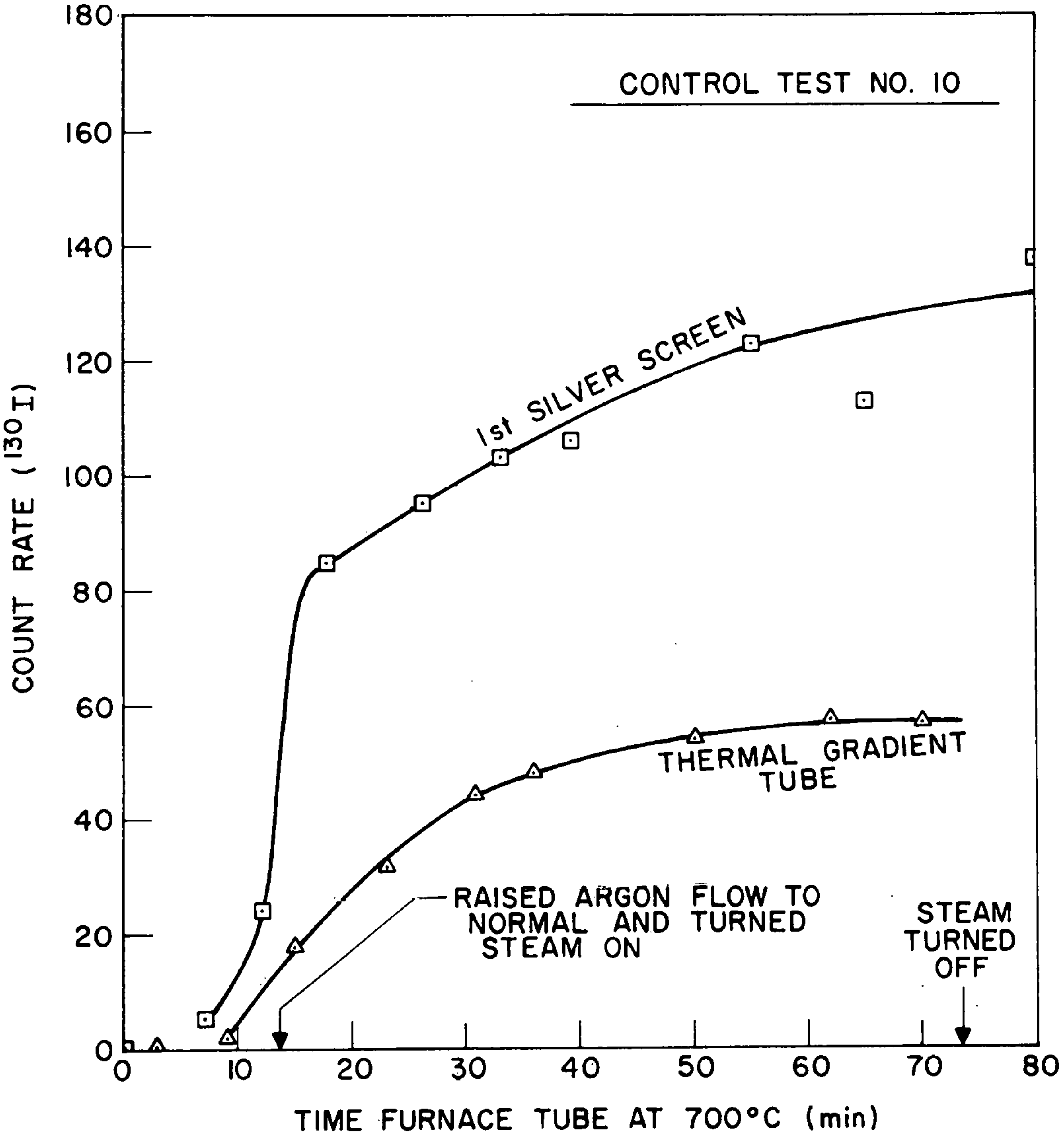

Fig. 3. Iodine-130 count rate of the thermal gradient tube and the first silver screen as a function of time. Control Test 10.

Although the significant decomposition of CsI which was noted in this test runs counter to the generally regarded[5] stability of CsI, we hasten to point out that the high release of iodine is unquestionably due to reaction of the molten CsI with the quartz boat, and the consequent formation of cesium silicates.

3. IMPLANT TESTS

3.1 Development of an Implantation Technique

Because of the costs and experimental difficulties associated with the use of fully irradiated fuel in studies of fission product behavior, most researchers seek to develop fuel preparation methods and experimental techniques which simulate as closely as possible typical conditions. Although the extent to which the simulant accurately corresponds to the actual situation is open to examination, a recent review[6] of the use of simulants vis-a-vis irradiated fuel has concluded that, if essential differences in fission product behavior are indeed present, these are insignificant when viewed in terms of the sensitivity to experimental conditions. It must be kept in mind, however, that this conclusion applies strictly to conditions of meltdown, wherein the high temperatures involved tend to minimize the importance of kinetics in determining chemical form.

Similarly for reasons of experimental convenience and economy, we have sought to develop a method to simulate fission product behavior in the fuel-clad gap of irradiated fuel. The objective was to distribute the fission product simulants on the surfaces of the UO_2 pellets, since additional release from the pellet matrix is inconsequential under the present set of test conditions.

A typical Implant Test fuel rod is sketched in Fig. 4; the method of implanting the fission products is outlined in the figure as well. Note that three pellets at each end of the test fuel rod were not treated so that axial migration within the fuel rod could be examined.

Only CsI was employed in Implant Tests 1 and 2, whereas the remaining tests performed to date utilized cesium as both CsI and CsOH. Cesium iodide which contained approximately 10% I-129 was first irradiated to provide the Cs-134 and I-130 radiotracers. The crystalline CsI

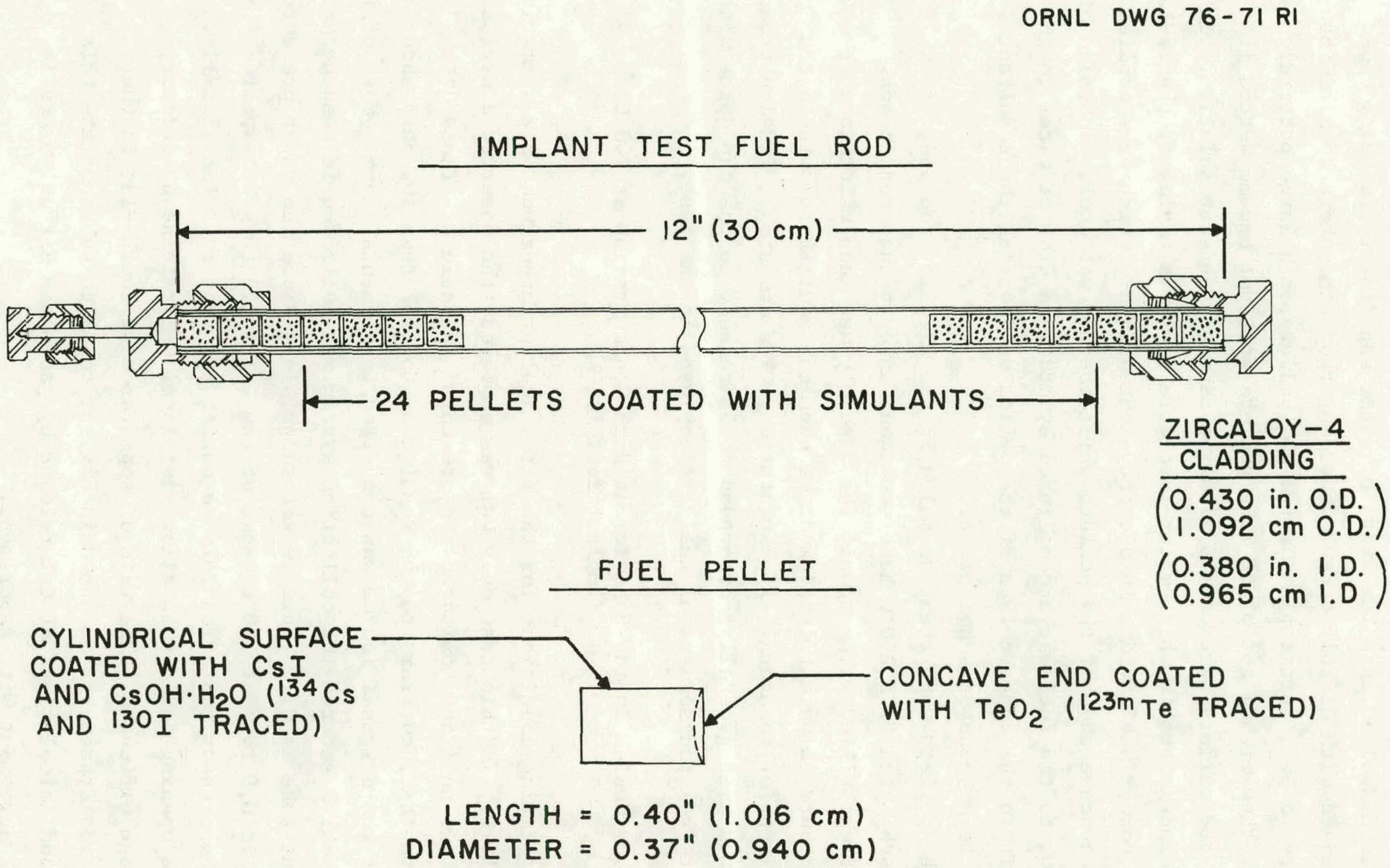

Fig. 4. Implant test fuel rod.

was then dissolved in a few drops of water and (for tests using CsOH also) mixed with dissolved CsOH under an argon atmosphere to minimize exposure to CO_2. After placing the UO_2 pellets on a large petri dish and heating them with a hot plate (the pellets will not become wetted if cool), the pellets were coated with the simulant aqueous solution. In those experiments in which water-insoluble TeO_2 was employed, the Te-123m traced powder was divided into twenty-four aliquots which were applied to the concave ends of the pellets while the UO_2 was cool. Adhesion of the TeO_2 to the fuel was accomplished by adding a drop of water to the TeO_2 within the concave face of the pellet and heating the resultant slurry to dryness on a hot plate.

The pellets were then assembled in the Zircaloy rod and, after being subjected to a 200°C heat treatment under vacuum conditions, the rod was filled with argon. The assembly was then maintained at 400°C for 16 hours to permit attainment of chemical equilibrium within the assembly prior to actual experimentation. The amounts of fission product simulants used generally correspond to 5% release to the gap space within a spent fuel rod segment of the size employed in the test.

3.2 Cesium Iodide Behavior at High Concentration at 700°C (Implant Test 1)

Operating conditions for the first implant experiment are summarized in Table 1. In this test only CsI was employed; the observed distributions of the two nuclides monitored are presented in Table 2. These data indicate that, contrary to the results of Control Test 10, only about 1.4% of the original iodine was converted to elemental form. Most of the cesium which entered the collection system was collected in the thermal gradient tube as CsI. This is not surprising, since the vapor pressure of CsI is 0.9 torr at 700°C; some of the CsI would thus be expelled with the pressurized argon release during rod rupture. The slit-like rupture opening could then allow additional CsI release by ordinary gas-phase diffusion. The rate of appearance of iodine-130 in the collection system, as is shown in Fig. 5, tends to substantiate this view, and calculations of CsI release by gas-phase diffusion are in nominal agreement with experiment.

ORNL DWG 76-141

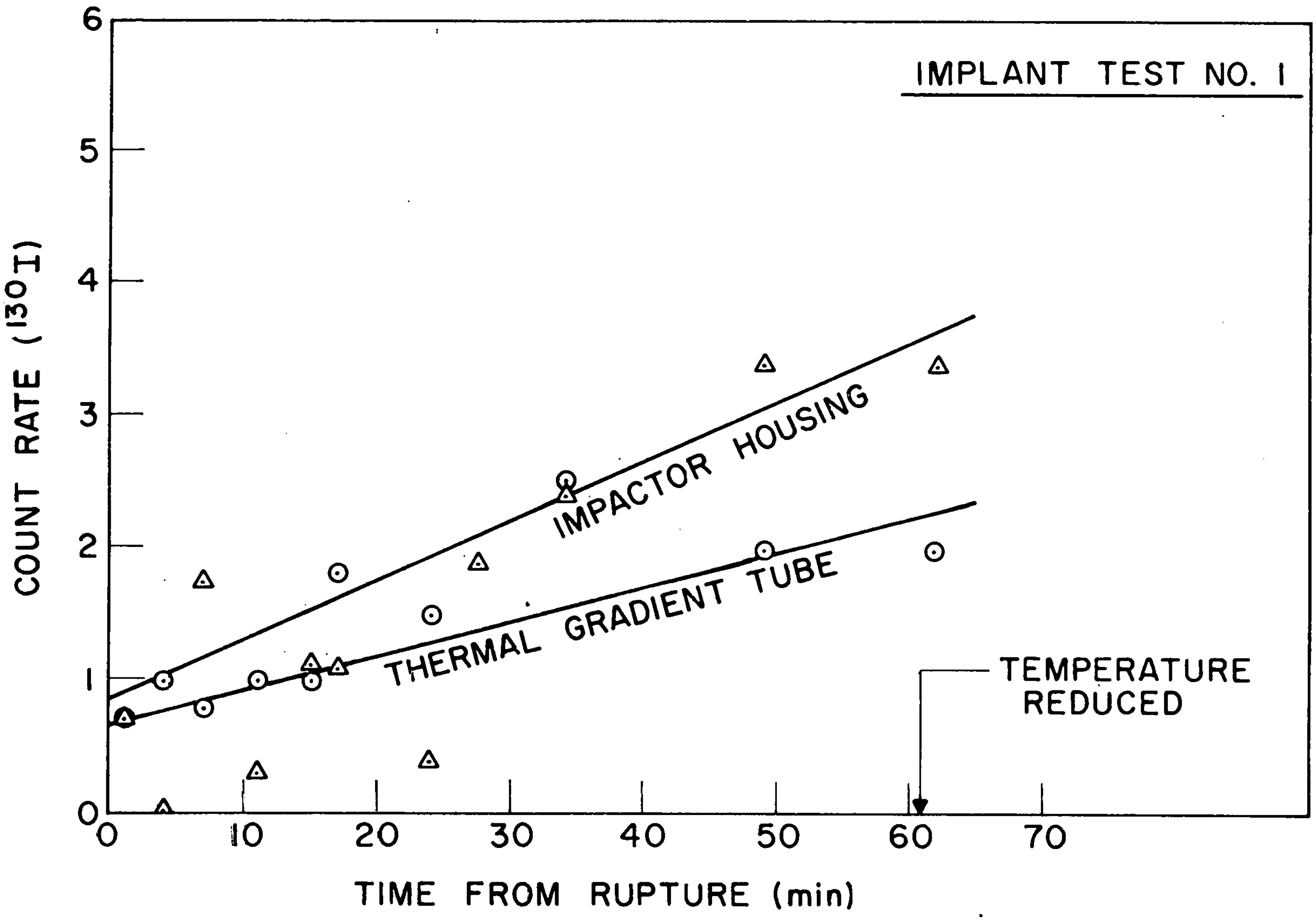

Fig. 5. Iodine-130 count rate of the thermal gradient tube and impactor assembly during Implant Test 1.

The distributions of the iodine-130 nuclide within the fuel rod, as determined before and after the experiment, are presented graphically in Fig. 6. Release of material in the immediate vicinity of the rupture area is unmistakable. Less well-defined is migration of the fission product simulant toward the cooler ends of the rod. The distributions presented in Fig. 6 probably represent CsI; this is substantiated by a comparison of the iodine-130 and cesium-134 scans which were made at the conclusion of the experiment. These data are shown graphically in Fig. 7.

A sample of material which was obtained from the collector of the fifth impactor stage (which collects the smallest aerosol particles) was submitted for X-ray diffraction analysis. Although the data of Table 2 suggest this material to be CsI, an examination of the diffraction pattern indicated that greater than 80% of the deposit was $CsOH \cdot H_2O$. The iodine apparently was not present in a form which could be detected by the X-ray diffraction technique.

3.3 Cesium Iodide Behavior at Low Concentration at 700°C (Implant Test 2)

Implant Test 2 was identical to the preceding test, except that a 70-fold lesser concentration of CsI was employed, and the test was run 30 min longer (cf. Table 1). The detailed distributions of the two nuclides monitored are presented in Table 2.

In this test 7.3% of the cesium and 16.5% of the iodine were released from the fuel rod, and about 14% of the original iodine was collected in elemental form. The cesium which deposited on the furnace tube walls was largely confined to an area near the tube rupture location, as might be expected if rapid condensation of the escaping species had occurred.

Deposition of the iodine in the impactor assembly and on the first silver screen during the course of the experiment is shown in Fig. 8. The data indicate some delay in the appearance of iodine on the silver screen; this may be due to holdup of the iodine on the aluminum impactor housing. Note also the apparent cessation of iodine release approximately 60 minutes following tube rupture.

ORNL DWG 76-149

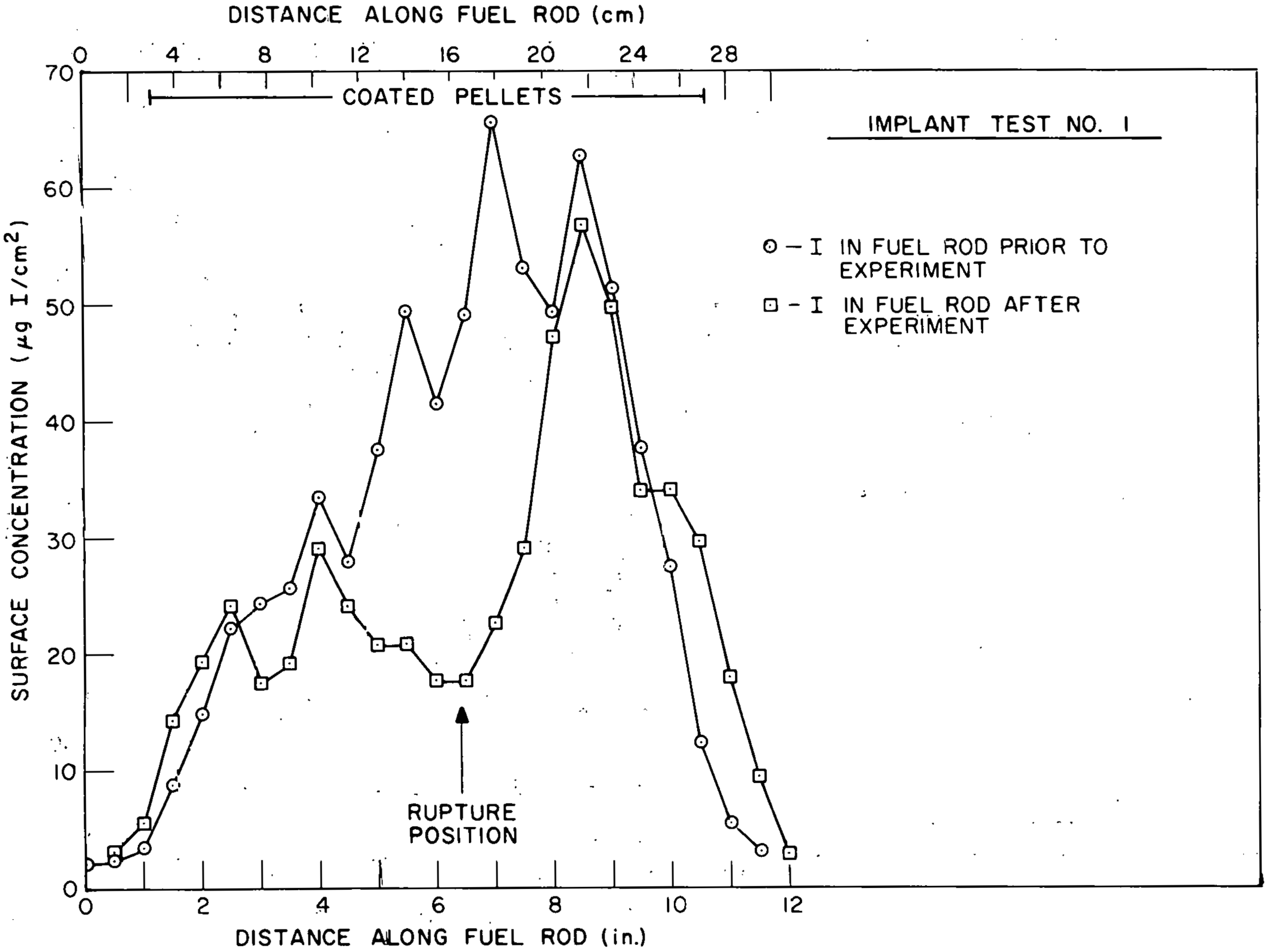

Fig. 6. Iodine-130 distributions in Implant Test 1 fuel rod.

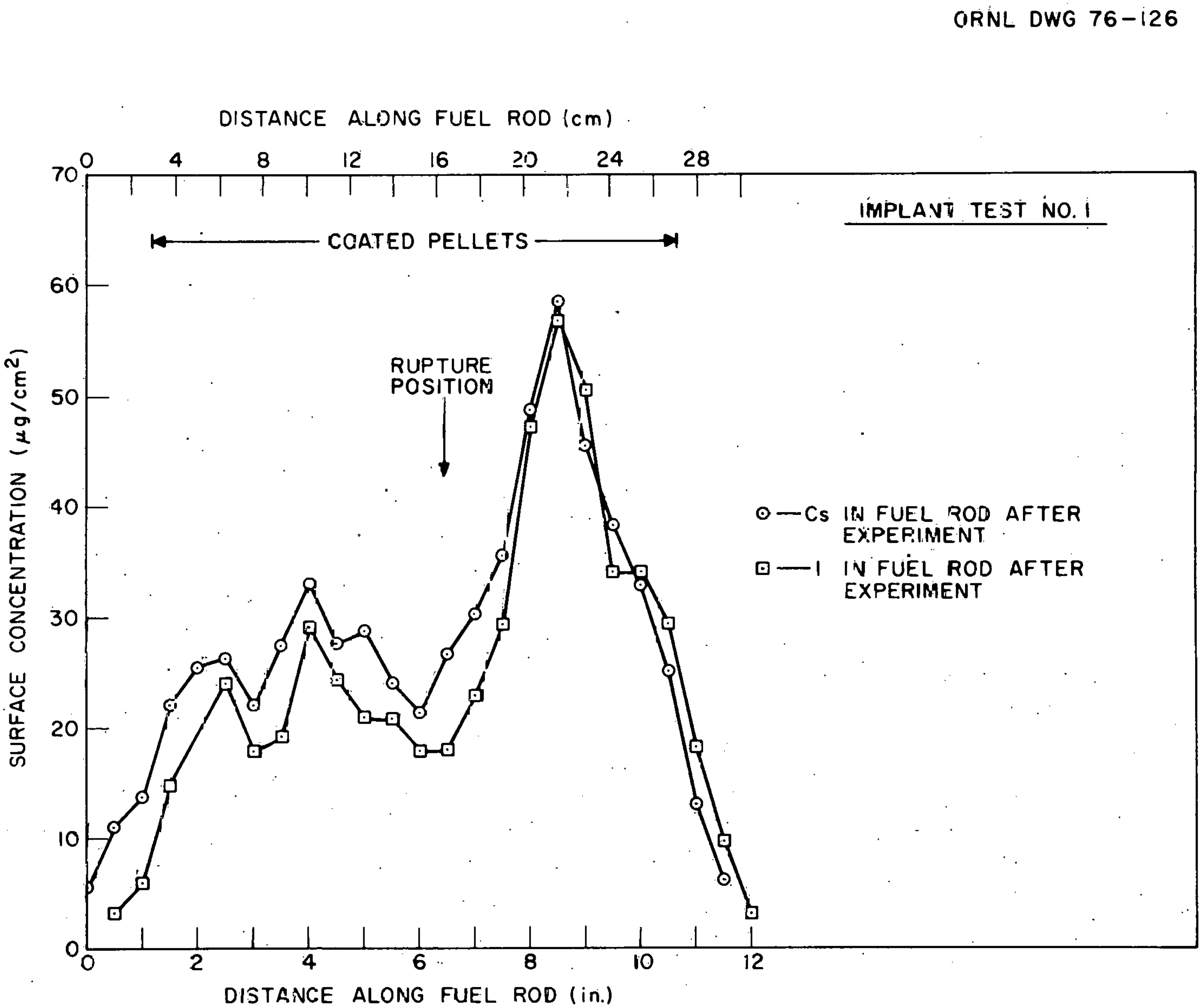

Fig. 7. Iodine-130 and cesium-134 distributions in Implant Test 1 fuel rod at conclusion of experiment.

ORNL DWG 76-152

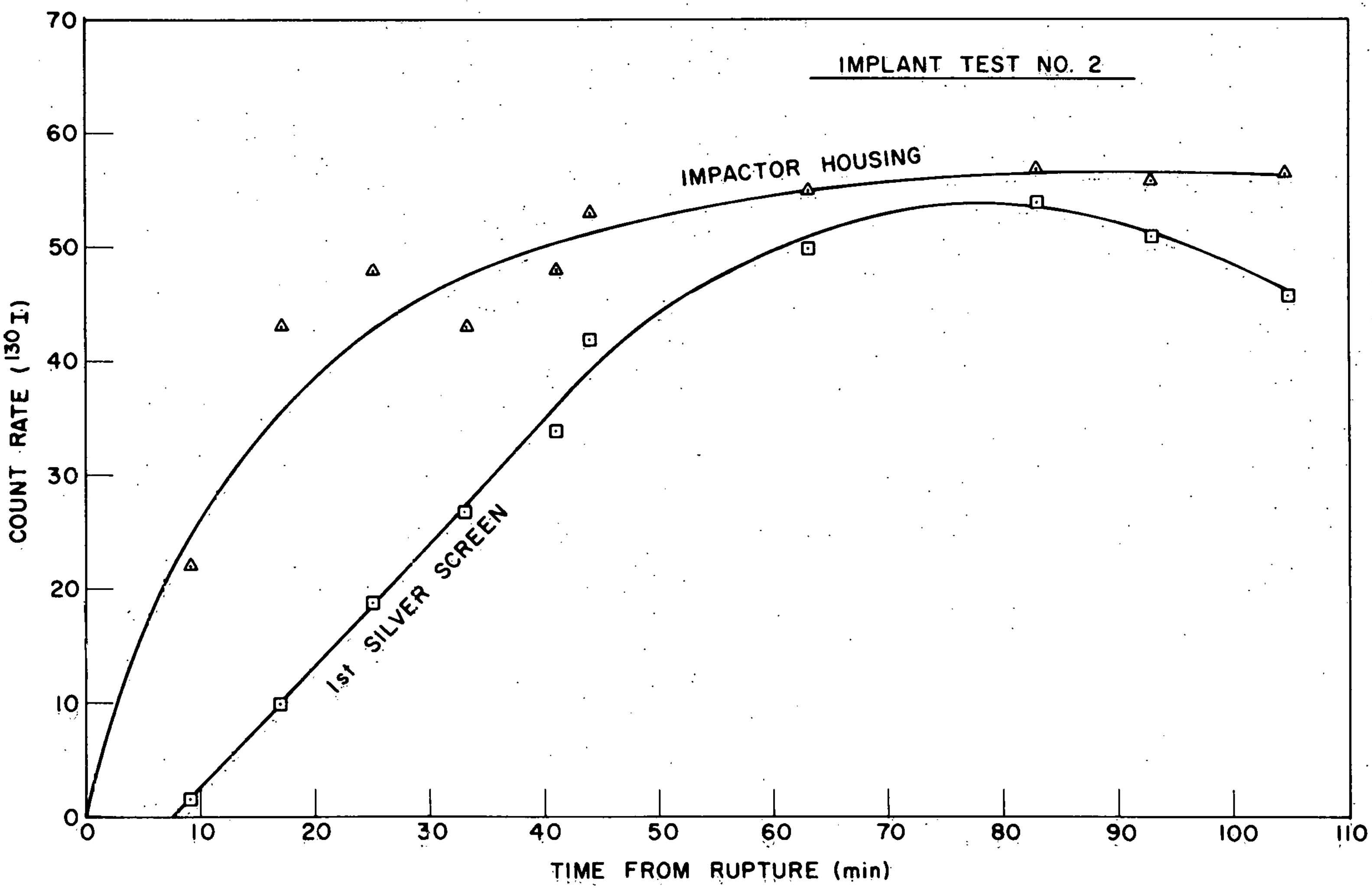

Fig. 8. Iodine-130 deposition in the impactor and on the first silver screen during Implant Test 2.

Cesium nuclide distributions in the fuel rod prior to and after experimentation are presented in Fig. 9. As in the previous test, these data indicate loss of material near the rupture point (5.6 inches along the fuel rod) and some migration to the ends of the fuel rod.

Particulate material from two impactor stage collectors was submitted for X-ray diffraction analysis. One of the samples from Stage 1 (which contained the highest amount of radioactivity) was found to be principally $CsOH \cdot H_2O$; the second sample, from Stage 4 (which contained the darkest visible deposit), was found to consist of almost equal amounts of $CsOH \cdot H_2O$ and $CsOH \cdot xH_2O$ ($x > 1$). Since the samples are exposed to air prior to X-ray analysis, the significance of the degree of hydration of the CsOH does not warrant further analysis at this time. Moreover, as remarked previously regarding similar results from Implant Test 1, the iodine on the collector stages was not in a form that could be detected by our diffraction technique.

The larger fractional formation and release of elemental iodine experienced in this test compared with Implant Test 1 were probably the manifestation of a concentration effect. In like manner, a larger proportion of iodine appeared as organic iodides (i.e., collected on the sorbers beyond the silver screens) in this test as compared with the previous test, again probably because of the differences in concentration. Such concentration effects on organic iodide formation have been noted previously.[7]

3.4 Tellurium Dioxide, Cesium Iodide, and Cesium Hydroxide Behavior at 900°C (Implant Test 3)

Implant Test 3 is the first of several experiments which will employ three fission product simulants. The experimental conditions are listed in Table 1, and the pertinent nuclide distributions at the conclusion of the test are presented in Table 3. The rupture area of the cladding is depicted in Fig. 10.

Cesium concentration profiles in the fuel rod are displayed in Fig. 11; these data indicate migration to the cold ends <u>and</u> to the rupture area. Moreover, migration to the rupture area appears to be due to a loss of cesium from the pellet surfaces in this region and a consequent reaction between this cesium and the cladding. Corresponding profiles for iodine, shown in Fig. 12, suggest migration as CsI toward the ends

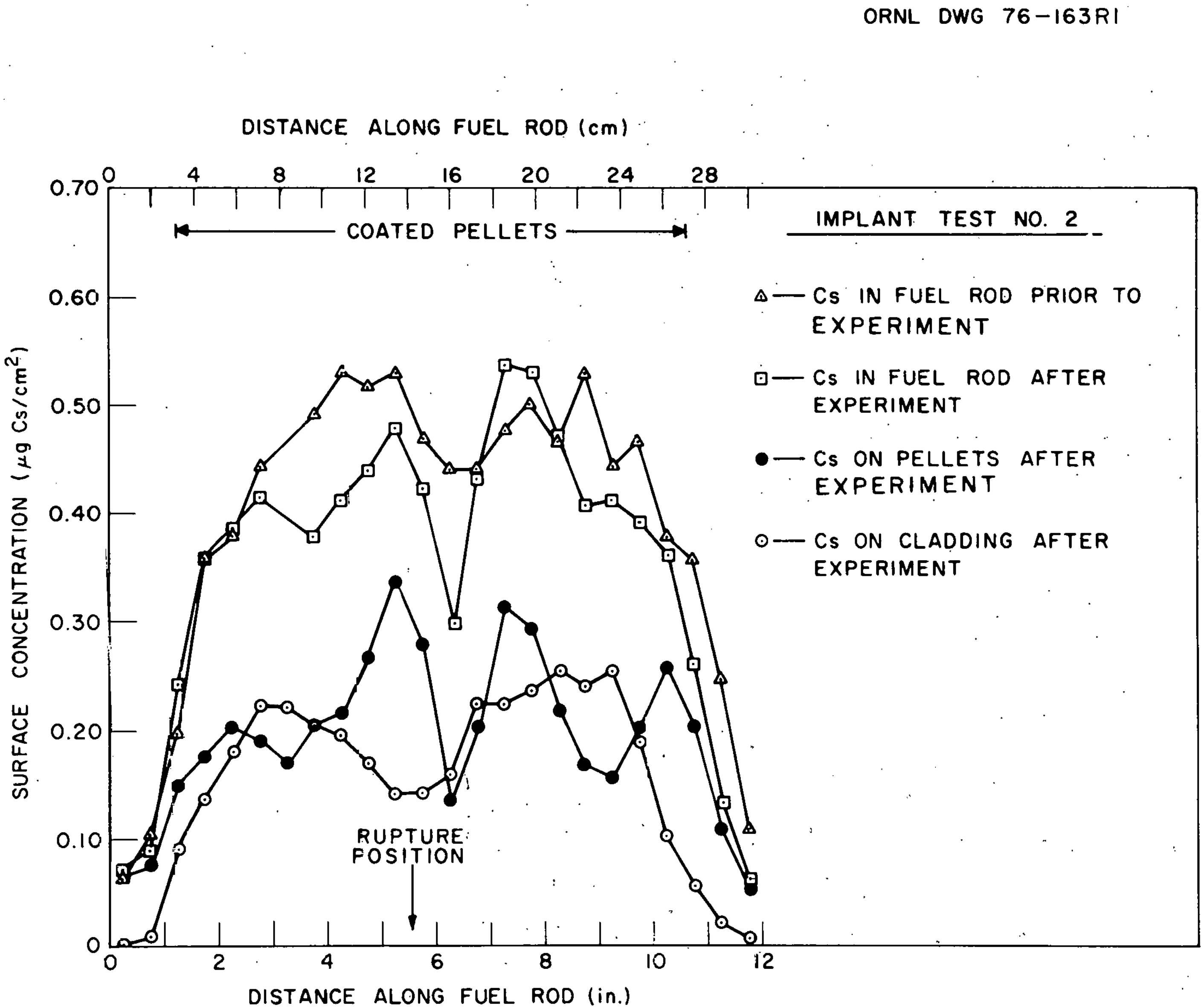

Fig. 9. Cesium-134 distributions in Implant Test 2 fuel rod.

Table 3. Distributions of cesium, iodine, and tellurium in Implant Test 3

Location	Temperature (°C)	Percent found in each location Cs	I	Te
UO_2 pellets	900	75.7	56.5	3.6
Zircaloy cladding	900	19.4	18.0	94.8
Quartz furnace tube	∿ 500	4.1	24.0	1.6
Thermal gradient tube	750–150	0.68	0.73	0.0003
Orifice assembly	125	0.014	0.08	0.0005
Impactor housing	125	0.032	0.52	0.00
First stage paper		0.006	0.02	0.0
Second stage paper		0.002	0.001	0.0
Third stage paper		0.002	0.001	0.0
Fourth stage paper		0.005	0.009	0.0
Fifth stage paper		0.012	0.038	0.0
Filter housing	125	0.001	0.043	0.001
First filter paper		0.003	0.004	0.0005
Second filter paper		0.0	0.001	0.0
Third filter paper		0.0	0.0006	0.0003
Silver screen No. 1		0.0	0.11	0.0
Silver screen No. 2		0.0	0.002	0.0
Silver screen Nos. 3-8		0.0	0.002	0.0
Adsorber housing	125	0.004	0.002	0.002
Charcoal No. 1		0.0004	0.006	0.0
Charcoal No. 2		0.0003	0.0	0.0
Other adsorbers		0.0008	0.0002	0.0
Condenser housing	0	0.04	0.0	0.0
Condensate		0.001	0.0	0.0
Freeze trap	−78	0.001	0.0	0.0
Cold charcoal trap	−78	0.0	0.0	0.0

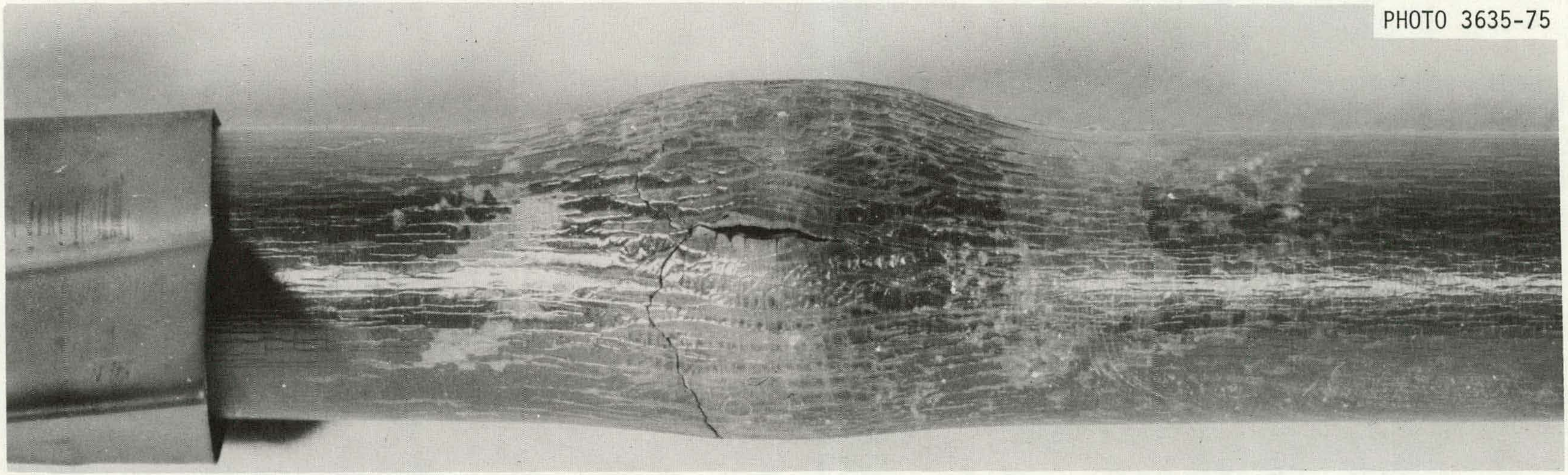
PHOTO 3635-75

Fig. 10. Implant Test 3 cladding in the region of rupture.

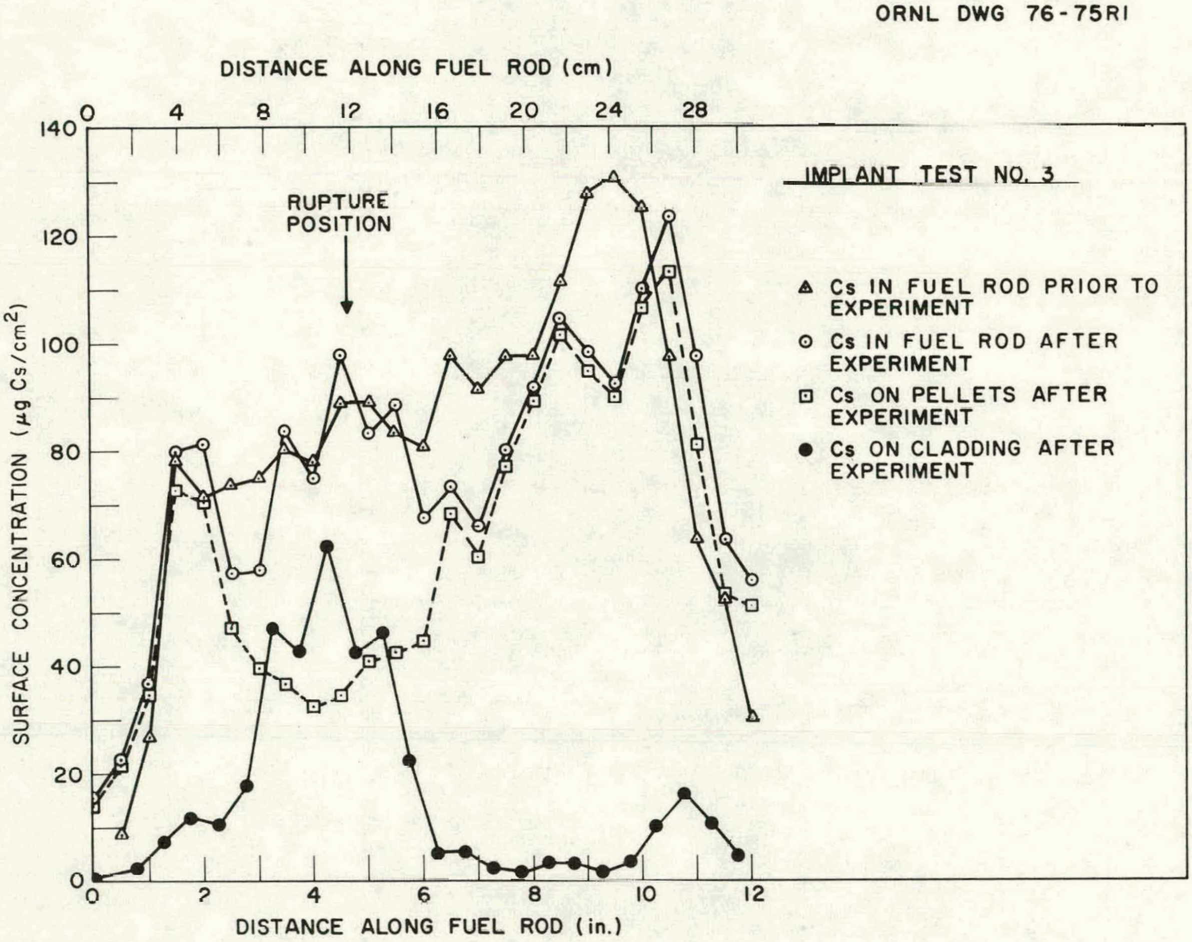

Fig. 11. Cesium-134 distributions in Implant Test 3 fuel rod.

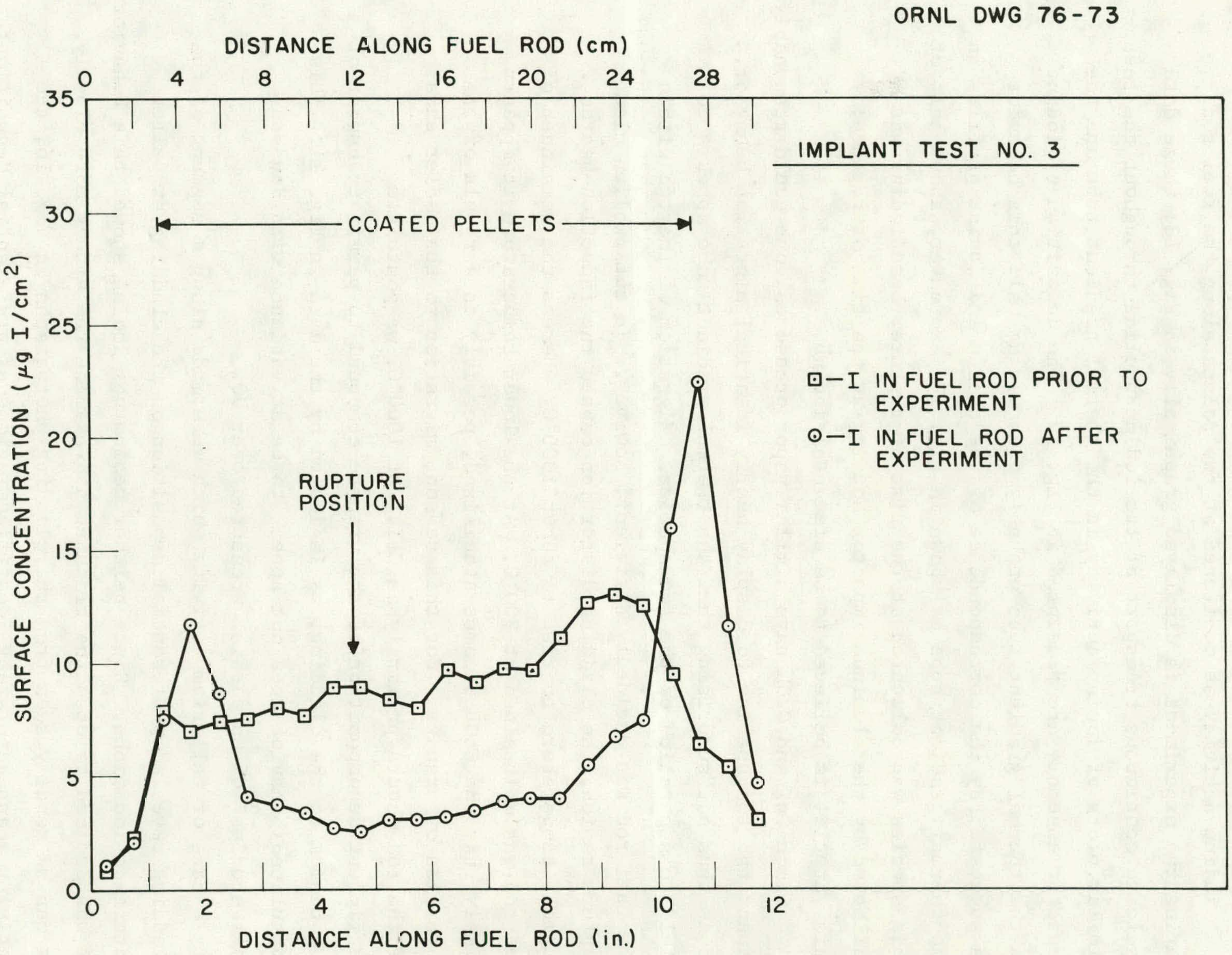

Fig. 12. Iodine-130 distributions in Implant Test 3 fuel rod.

of the rod, and migration of the cesium originally associated only with CsOH in the rupture region.

Iodine activity as monitored at two points along the fuel rod during the experiment is displayed graphically in Fig. 13; these data indicate continuous transport of the iodine nuclide throughout the test. Similar plots of iodine activity in the thermal gradient tube and the impactor assembly are presented in Fig. 14. The deposition of iodine in the thermal gradient tube probably occurred as CsI; this behavior is suggested by the correspondence of the cesium and iodine profiles in the thermal gradient tube as shown in Fig. 15. Moreover, about half of this species was collected at the time of rupture. Less iodine was collected by the aluminum impactor housing at the time of rupture; this material is believed to be elemental iodine.

Since CsI and CsOH have similar vapor pressures, one could reasonably expect the two species to display nearly identical migration behavior. It is thus not surprising that the thermal gradient tube appears to yield no separation of the two species. Migration of the two within the fuel rod was decidedly different, however. In the swollen clad rupture region, the cladding distortion caused the induction-heated segment temperature to rise to about 1000°C, whereas the remainder of the rod was maintained at 900°C. At the lower temperature it appears likely that the CsOH becomes stabilized, possibly as a result of the formation of uranate. For this reason, migration to the cooler ends of the rod occurs primarily as CsI. At 1000°C, we postulate sufficient decomposition of the uranate compound to permit transport of the cesium to the cladding, as indicated by the data in Fig. 11. This postulated behavior does not appear to be at variance with Knudsen cell studies[2] of Cs partial pressures over UO_2.

Scans of tellurium activity which were made along a segment of the cladding revealed preferential deposition on the cladding at pellet interface locations. Since neither cesium nor iodine showed this behavior, it was decided to open the cladding and examine the effect more closely. As can be readily seen from the cladding photographs in Fig. 16, the activity scans accurately identified regions of preferential deposition; the tellurium species obviously did not distribute uniformly along the fuel rod. Samples of material removed from the regions of tellurium-clad

ORNL DWG 76-72

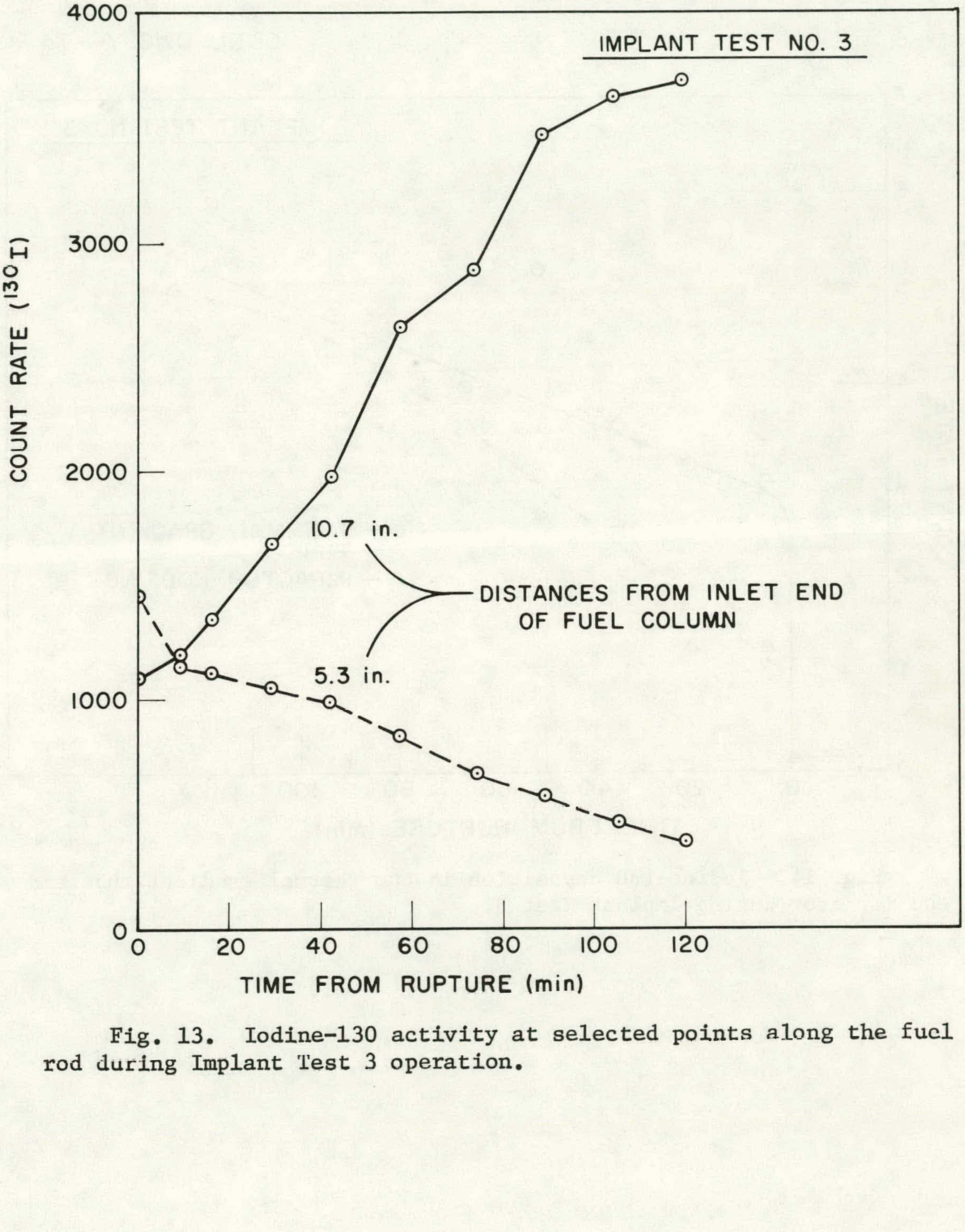

Fig. 13. Iodine-130 activity at selected points along the fuel rod during Implant Test 3 operation.

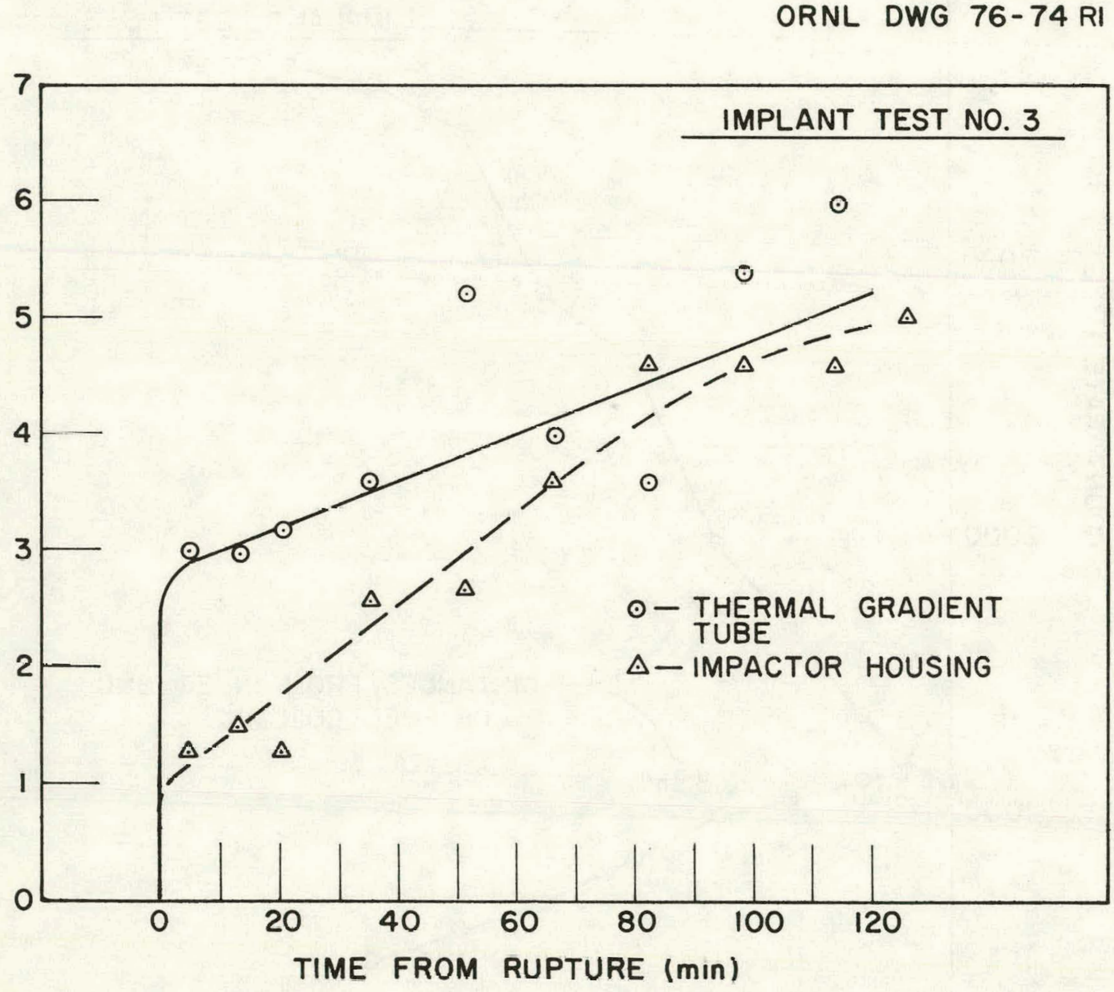

Fig. 14. Iodine-130 deposition in the thermal gradient tube and the impactor during Implant Test 3.

ORNL DWG 76-70

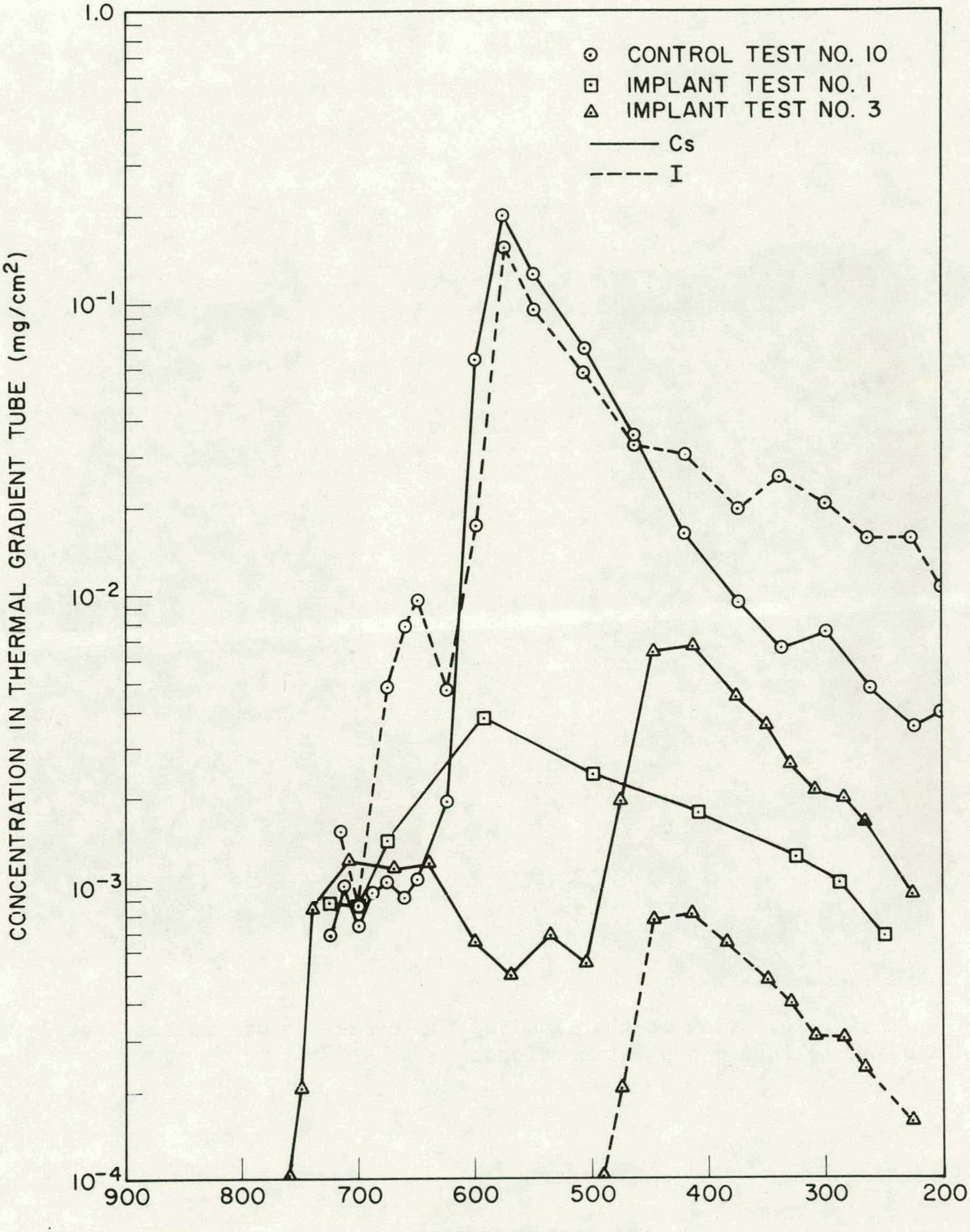

Fig. 15. Cesium-134 and iodine-130 profiles in the thermal gradient tube.

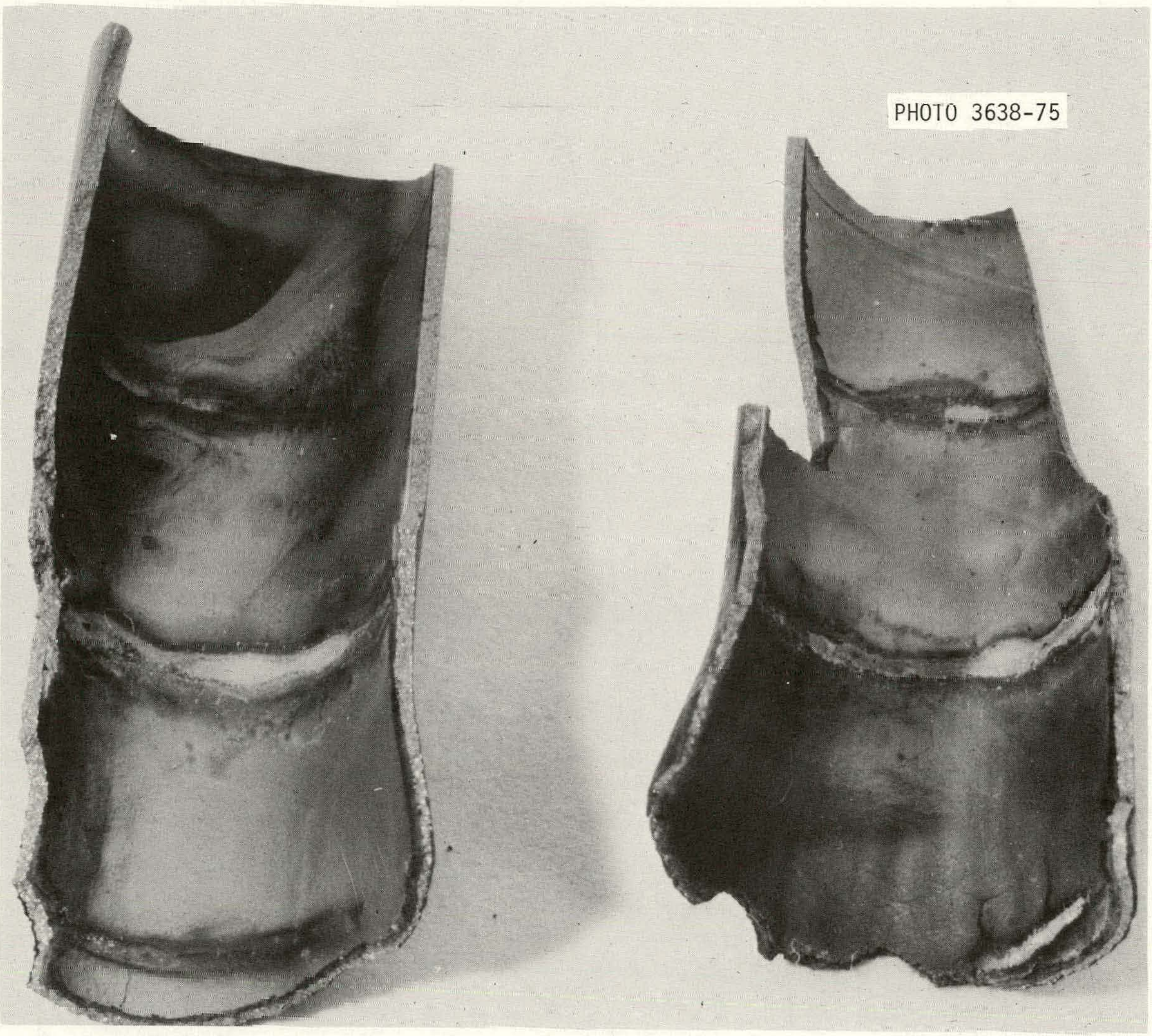

Fig. 16. View of the cladding inner surface of Implant Test 3 showing tellurium deposition rings.

interaction exhibited X-ray diffraction patterns which could not be identified.

3.5 Behavior of Fission Product Simulant Mixture at 1100°C (Implant Test 4)

Implant Test 4, which was conducted over a one-hour period with the fuel rod maintained at 1100°C, was similar to Implant Test 3 in simulant makeup and composition.

A lengthened induction coil was employed to reduce the axial temperature gradient along the fuel rod. However, this caused the stainless-steel ferrule fitting at the inlet end of the rod to become overheated; this resulted in leakage of the argon pressurizing gas, so that rupture of the rod could not be effected. Nonetheless, approximately 18% of the cesium, 32% of the iodine, and 0.1% of the tellurium were released. Most of the iodine deposited on the furnace tube wall near the entrance to the thermal gradient tube, probably as CsI. Considerable migration of iodine was observed within the fuel rod toward the cooler ends and, although virtually all of the tellurium migrated to the cladding, the deposition rings which were observed in Implant Test 3 were noticeably absent.

Oxidation of the Zircaloy cladding at 1100°C produced smoke-like deposits on the furnace tube wall that ranged in color from black to white. The orifice at the entrance to the impactor became partially plugged by ZrO_2 particulates (as determined by X-ray diffraction); this necessitated reduction of the steam-argon flow. Moreover, post-test examination of the cladding revealed it to be very brittle, and the surface flaky.

More detailed analysis of the experiment is presently underway.

3.6 Behavior of Fission Product Simulant Mixture at 700°C (Implant Test 5)

Implant Test 5 was similar to Implant Test 3 in terms of the nature and compositions of the simulants, but was conducted instead at 700°C over a two-hour period. As with Implant Test 4, data analysis is incomplete.

The data examined to date indicate that about 4% of the cesium, 15.5% of the iodine, and 6% of the tellurium had been released, and that most of this occurred at the time of rupture. Because a different method of wall thinning was attempted for this test, the rupture was more energetic than experienced in the previous tests. Approximately 500-psi argon pressure was required to burst the rod in this test compared with 330 psi in Implant Tests 1 and 2, and 250 psi in Implant Test 3. (Wall thinning is necessary for tests at temperatures at or below 700°C to prevent breakage of the quartz furnace tube.)

4. PREPARATION OF HIGH-BURNUP FUEL ROD SPECIMENS

The capped segments of H. B. Robinson 2 fuel rods have been received in good condition from Battelle Columbus Laboratories (BCL). Six of these segments have been selected for experimentation and have been transported to a hot cell, where detailed scans will be made to determine the axial concentration profiles of selected gamma-emitting fission products.

The following description of operations which had been performed at the Battelle Columbus Laboratories is taken from correspondence of R. W. Klingensmith.[8] The two subject rods were received at the BCL Hot Laboratory as part of a shipment of 20 H. B. Robinson 2 fuel rods from Aerojet Nuclear Company (ANC) in Idaho. The rods were removed from the fuel assembly at the ANC facility in Idaho.

4.1 Fission Gas Analysis

Accumulated fission gases within each rod were collected and then analyzed by mass spectrometry for molecular and isotopic constituents. A determination was also made of the total amount of gas and the void volume within each rod.

Gases were collected from the fuel rod using an in-cell puncturing device and an out-of-cell collection system. Operationally, a fuel rod is inserted through a gas-tight punch chamber which, along with the out-of cell collection system, is evacuated. The clad is then punctured and the gas allowed to expand into a calibrated volume. The resulting pressure in this volume is measured with a sensitive Wallace-Tiernan pressure gage, and the gas quantity calculated using the ideal gas law.

The gas is then expanded a second time into a calibrated volume for a second measurement. The void volume of the fuel rod is determined as the difference between pre-puncture and post-puncture system volumes. In order to determine the statistical spread of the values, ten measurements are made before and after puncturing. To assure complete filling of the rod internal volume, helium at high pressures is utilized in the system.

Pertinent data and the results of the gas analyses are presented in Tables 4 through 6. (These data indicate only 0.24% release to the gap and plenum, as reported previously.[2]) A special effort was made to detect methyl iodide. For both rods, methyl iodide content was below the 0.1 ppm detection limit.

4.2 Marking and Sectioning

Overall dimensions of the fuel rods examined were 152 in. long by 0.422 in. OD. Each rod was marked (± 1/16 in.), starting from the bottom, at 12, 24, 48, 60, 72, 84, 96, 120, and 132 in. The area one inch on either side of each mark was cleaned using a wire brush. Visual inspection of each cleaned area assured that no debris remained that would hinder Swagelok sealing. A tubing cutter was used to section the rods at each of the marks. From each rod ten pieces of length (in order from the bottom) 12, 12, 24, 12, 12, 12, 12, 24, 12, and 20 inches were obtained. In all cases the cutting operations resulted in a negligible amount of fuel falling from any of the cut surfaces.

Immediately upon cutting, the exposed-fuel ends of each section were sealed with stainless steel Swagelok fittings. The upper end of each section was sealed with a Swagelok cap fitting which has a 2-in. length of 1/8-in.-OD stainless tubing welded into a hole through the cap. A 1/8-in. Swagelok cap fitting was used to seal the 1/8-in. tube. The lower end of each section is sealed with a regular Swagelok cap fitting. The two end sections of each rod are sealed with the fittings which have the 1/8-in. tube attachment. Special stainless steel ferrules were fabricated for these fittings to assure positive seal to the 0.422-in.-diameter rod. This method of sealing was verified by performing a helium leak check at 80 psi on a sample system.

Table 4. Fission gas results of the H. B. Robinson 2 fuel rods

		First expansion			Second expansion				Void volume		
Rod No.	Avg. punch temp. (°C)	Puncture volume V_2 (cc)	Puncture volume pressure P_2 (psia)	Gas quantity V_{t1} (cc, STP)	Volume after expansion V_{2S} (cc)	Pressure after expansion P_{2S} (psia)	Gas quantity V_{t2} (cc/STP)	Average gas quantity (cc, STP)	Post-punch volume V_2 (cc)	Pre-punch volume V_1 (cc)	Rod void volume V_v (cc)
D-12	25.7	507.5	11.800	372.4	721.2	8.285	371.5	372.0	493.81±0.10	467.32±0.07	26.49±0.21
H-15	24.3	508.7	11.718	372.4	722.4	8.230	371.4	371.9	495.00±0.09	467.59±0.12	27.41±0.15

Table 5. Gas analyses of the H. B. Robinson 2 fuel rods

Rod No.	H_2	He	CH_4	H_2O	O_2	N_2	Ar	CO_2	Kr	Xe	Xe/Kr
D-12	< 0.01	95.2	0.01	< 0.1	< 0.27	1.27	2.05	< 0.01	0.133	1.04	7.82
H-15	< 0.01	95.2	0.01	< 0.1	< 0.49	2.04	0.91	< 0.01	0.158	1.18	7.47

Table 6. Krypton and xenon isotopic analyses of the H. B. Robinson 2 fuel rods

	Isotopic abundance (%)								Mass spectrometer		
Rod	Krypton				Xenon				Volume	pressure	Temp.
No.	83	84	85	86	131	132	134	136	cc	mm Hg	(°C)
D-12	13.7	31.1	7.17	48.0	7.86	21.0	28.9	42.4	1104.2	132	24.1
H-15	13.7	30.8	7.67	47.9	8.10	21.0	28.9	42.0	1147.7	128	24.0

For identification purposes, Rod D-12 is designated "A" and Rod H-12 is designated "B". Sections from each rod were numbered 1 through 10 starting at the bottom end of the fuel rod. Thus the sections are identified as A-1 through A-10 and B-1 through B-10. These identification marks are etched on each of the Swagelok fittings.

A period of approximately 90 days elapsed between the time the rods were punctured for fission gas analysis and the time they were sectioned. During this interval an air-tight seal was placed over the small puncture hole in the clad. It should be pointed out that the interior of Rod A (D-12) was exposed to air through the gas vent hole for about 72 hrs before the hole was sealed. Rod B (H-15) was similarly exposed for about 48 hrs.

4.3 Packaging and Shipping

The rod sections were individually placed in stainless steel tubes, and these tubes, in turn, were placed in stainless steel tubes which were tack-welded together into a cluster to form a shipping basket. Spring-loaded stainless steel cylinders were placed into each of the shipping basket tubes to constrain movement of the fuel rod sections during transport. The entire shipping basket assembly was then placed in a stainless steel, water-tight shipping cannister and transported in this configuration.

As indicated previously, all of the rod sections were received in good condition at ORNL.

5. KNUDSEN CELL EXPERIMENTS

As a result of the X-ray diffraction studies associated with the Control and Implant Tests, it is now apparent that the species previously identified as Cs_2O_2 in the Knudsen cell tests[2] is actually hydrated CsOH. The characteristic heat of vaporization which was determined for Cs vapor over the $CsOH \cdot xH_2O-UO_2$ system by the Knudsen cell technique was 60.4 kcal/mole; this result is in good agreement with the values of 63.4 and 69.6 kcal/mole which were obtained for Cs vapor over Cs_2UO_4 by Johnson and Johnson.[9] These workers, in agreement with the present observations, detected minor ion currents of CsO^+,

Cs_2O^+, and Cs_2^+, but no species which contained uranium. These data reinforce our conjecture that the Cs_2CO_3 and the $CsOH{\cdot}H_2O$ reacted with excess UO_2 in the Knudsen cell to yield Cs_2UO_4, so that the effusing cesium corresponded to the vapor pressure in equilibrium with the uranate. An orange-red compound that remained in the Knudsen cell after studies with a Cs_2CO_3-UO_2 mixture has been submitted for analysis by X-ray diffraction.

In an effort to convert the ion current-temperature products into vapor pressure values, calibration of the Knudsen cell-double focusing mass spectrometer apparatus has been attempted using silver as a standard. After several unsuccessful attempts, each of which resulted in apparatus adjustments to correct malfunctions, a satisfactory calibration curve was obtained. This curve yielded a heat of vaporization value of 61 kcal/mole, which is in essential agreement with values (63 to 69 kcal/mole) reported previously.[10,11]

REFERENCES

1. Quarterly Progress Report on Reactor Safety Programs Sponsored by the NRC Division of Reactor Safety Research for April-June 1975, ORNL-TM-5021, pp. 99-104, September 1975.

2. A. P. Malinauskas et al., Quarterly Progress Report on Fission Product Release from LWR Fuel for the Period July-September 1975, ORNL-TM-5143, November 1975.

3. Quarterly Progress Report on Reactor Safety Programs Sponsored by the NRC Division of Reactor Safety Research for October-December 1974, ORNL-TM-4805, Vol. 1, pp. 111-113, April 1975.

4. J. C. Bailar, Jr., Comprehensive Inorganic Chemistry, Vol. 1, pp. 467-69, Pergamon, New York, 1973.

5. B. D. Epstein, A Review of Literature Pertinent to Fission Product Migration and Interaction in Fuel Rods, GA-A13423, June 1975.

6. A. P. Malinauskas, "Use of Simulants for Fission Product Release," paper presented at the Second Light Water Reactor Safety Research Information Meeting, Sept. 19, 1974. See also Nuclear Safety 16, 19 (1975).

7. A. K. Postma and R. W. Zavadoski, Review of Organic Iodide Formation Under Accident Conditions in Water-Cooled Reactors, WASH-1233, October 1972.

8. R. W. Klingensmith, private communication with R. A. Lorenz, November 19, 1975.

9. C. E. Johnson and I. Johnson, Reactor Development Program Progress Report, ANL-RPP-3, p. 5.2, October 1972.

10. M. B. Parrish, J. Chem. Eng. Data 6, 592 (1961).

11. R. A. Rapp, Techniques of Metals Research, Vol. IV, Part 1, "Physicochemical Measurements in Metals Research," Interscience, New York (1970), p. 509.

ORNL/TM-5290
NRC-1, -3

Internal Distribution

1. M. Bender
2. C. J. Borkowski
3. K. B. Brown
4. J. R. Buchanan
5. J. B. Cathcart
6. R. H. Chapman
7. C. F. Coleman
8. W. B. Cottrell
9-14. J. L. Collins
15. F. L. Culler
16. G. G. Fee
17. D. E. Ferguson
18. M. H. Fontana
19. D. O. Hobson
20. H. W. Hoffman
21. G. Hofmann
22-25. R. A. Lorenz
26. F. C. Maienschein
27-36. A. P. Malinauskas
37. S. R. Manning
38. D. L. McElroy
39. C. J. McHargue
40. F. H. Neill
41-42. M. F. Osborne
43. G. W. Parker
44. H. Postma
45. D. G. Thomas
46. D. B. Trauger
47. J. R. Weir
48. R. G. Wymer
49-50. Central Research Library
51. Document Reference Section
52. Laboratory Records - RC
53-57. Laboratory Records Department
58. ORNL Patent Section
59. W. K. Davis (Consultant)
60. J. C. Frye (Consultant)
61. C. H. Ice (Consultant)
62. J. J. Katz (Consultant)
63. R. B. Richards (Consultant)

External Distribution

64-71. Director, Division of Reactor Safety Research, Nuclear Regulatory Commission, Washington, DC 20555
72. Director, Reactor Division, ERDA, ORO
73. Director, Research and Technical Support Division, ERDA, ORO
74-393. Given distribution as shown in categories NRC-1, -3

☆ U.S. GOVERNMENT PRINTING OFFICE: 1976-748-189/289